Stem Cell Reports
Article

ISSCR

OPEN ACCESS

Osteomacs promote maintenance of murine hematopoiesis through megakaryocyte-induced upregulation of Embigin and CD166

Safa F. Mohamad,[1] Roy El Koussa,[1] Joydeep Ghosh,[2] Rachel Blosser,[3] Andrea Gunawan,[2] Justin Layer,[2] Chi Zhang,[4] Sonali Karnik,[2] Utpal Davé,[2] Melissa A. Kacena,[3,5] and Edward F. Srour[1,2,6,7,*]

[1]Department of Microbiology and Immunology, Indiana University School of Medicine, Indianapolis, IN, USA
[2]Department of Medicine, Indiana University School of Medicine, Indianapolis, IN, USA
[3]Department of Orthopaedic Surgery, Indiana University School of Medicine, Indianapolis, IN, USA
[4]Department of Medical and Molecular Genetics, Indiana University School of Medicine, Indianapolis, IN, USA
[5]Department of Anatomy, Cell Biology and Physiology, Indiana University School of Medicine, Indianapolis, IN, USA
[6]Department of Pediatrics, Indiana University School of Medicine, Indianapolis, IN, USA
[7]Lead contact
*Correspondence: esrour@iu.edu
https://doi.org/10.1016/j.stemcr.2024.02.004

SUMMARY

Maintenance of hematopoietic stem cell (HSC) function in the niche is an orchestrated event. Osteomacs (OM) are key cellular components of the niche. Previously, we documented that osteoblasts, OM, and megakaryocytes interact to promote hematopoiesis. Here, we further characterize OM and identify megakaryocyte-induced mediators that augment the role of OM in the niche. Single-cell mRNA-seq, mass spectrometry, and CyTOF examination of megakaryocyte-stimulated OM suggested that upregulation of CD166 and Embigin on OM augment their hematopoiesis maintenance function. CD166 knockout OM or shRNA-*Embigin* knockdown OM confirmed that the loss of these molecules significantly reduced the ability of OM to augment the osteoblast-mediated hematopoietic-enhancing activity. Recombinant CD166 and Embigin partially substituted for OM function, characterizing both proteins as critical mediators of OM hematopoietic function. Our data identify Embigin and CD166 as OM-regulated critical components of HSC function in the niche and potential participants in various *in vitro* manipulations of stem cells.

INTRODUCTION

Interactions between hematopoietic stem cells (HSC) and cells of the hematopoietic niche are important to maintain hematopoiesis. Among the cellular residents of the niche involved in this process is a group of bone-resident macrophages known as osteomacs (OM) (Chang et al., 2008; Mohamad et al., 2017; Winkler et al., 2010) and the bone-forming cells, osteoblasts (OB). We previously demonstrated that OM are present in digests of neonatal calvarial cells (NCC) and in long adult bones (Mohamad et al., 2017, 2021) of mice. OM and OB are involved in HSC maintenance (Chitteti et al., 2010a; Mohamad et al., 2017) through molecularly uncharacterized mechanisms that are significantly augmented by interactions with megakaryocytes (MK; Mohamad et al., 2017). We reported that OM share many properties with bone marrow (BM)-derived macrophages, including their lowest common denominator phenotype, $CD45^{+}F4/80^{+}$, but differ significantly phenotypically (Mohamad et al., 2017, 2021). Furthermore, the proliferation of BM-derived macrophages was not enhanced by MK and they could not functionally substitute for OM to augment hematopoietic function (Mohamad et al., 2017). We also described the physical separation of OM from BM-derived macrophages in murine long bones via the sequential harvest of marrow cells and enzymatic digestion of bone (Mohamad et al., 2017, 2021).

CD166 is an immunoglobulin superfamily (Lehmann et al., 1989) transmembrane glycoprotein that interacts with CD6 (Degen et al., 1998). We demonstrated that the loss of CD166 is detrimental to HSC function and damaging for the competence of the niche (Cheng et al., 2011; Chitteti et al., 2010a, 2010b, 2014). CD166 is expressed on other niche residents such as mesenchymal stem cells, endothelial cells, and OM (Chitteti et al., 2013a; Mohamad et al., 2017). Embigin, another immunoglobulin superfamily protein (Huang et al., 1990; 1993), is an ion transporter essential for transporting lactate into neurons (Wilson et al., 2013). Blocking Embigin in the niche resulted in the loss of quiescence and increased the frequency of progenitors plus long- and short-term HSC (Silberstein et al., 2016).

Here, we further characterize OM (Mohamad et al., 2017) and identify them as critical components of the niche using *in vitro* and *in vivo* studies. We report that crosstalk between OM, OB, and MK is required for the upregulation of CD166 and Embigin expression on OM. Once activated, these molecular mediators are partially responsible for the combined OM/OB-mediated enhancement of hematopoietic function. We define hematopoietic function in this study as the maintenance of or increase in hematopoietic output measured *in vitro* by clonogenic or *in vivo* by repopulating assays of cells cultured for 7 days.

RESULTS

Purity of collected macrophages and OM

A recent report (Millard et al., 2021) suggests that it is very difficult to obtain intact BM macrophages (or OM) in single-cell preparations because macrophages break into F4/80$^+$ membrane fragments and stick to all other cell types in the BM, rendering the purity of selected F4/80$^+$ cells dubious. We tested this by flow cytometry since one should not be able to find distinct T (CD3) or B (B220) cells that are also F4/80$^+$. Indeed, in all of the cell preparations examined, we did not encounter CD3$^+$F4/80$^+$ or B220$^+$F4/80$^+$ events to the tune of 60% of T cells as reported by Millard et al. (Figure 1). Fragments from macrophages attached to lymphocytes should have minimal or no effect on cell size (forward and side scatter) and no effect whatsoever on granularity (side scatter). Therefore, a discrete population of "contaminated" lymphocytes should be observed within the lymphocyte gate. As can be seen in Figure 1 and the associated bar graph, within the lymphocyte gate, discrete CD3$^+$F4/80$^+$, B220$^+$F4/80$^+$, or Ter-119$^+$F4/80$^+$ events could not be identified. We therefore consider our preparations of OM and macrophages sufficiently pure as expected from flow cytometric cell sorting and adequate to perform the subsequent work.

Comparative analysis of OM- and BM-derived macrophages

OM share multiple characteristics with BM-derived macrophages (Mohamad et al., 2017), including having the same common denominator phenotype, CD45$^+$F4/80$^+$. To characterize OM as best as we can, we pursued the further characterization of OM to find a unique genetic or phenotypic trait that distinguishes OM and assist us in generating a conditionally OM knockout (KO) mouse. We used multidimensional cytometry by time of flight (CyTOF) with 17 antibodies to examine fresh cells isolated from age-matched donors (Figure 2A). Studies with these 17 antibodies were repeated 3 times. Based on the collective and spatial distribution of gated CD45$^+$F4/80$^+$ events with respect to one another in the ViSNE plots between the left and right columns in Figure 2A, fresh neonatal OM and macrophages are phenotypically discrete and are distinct from one another. Interestingly, OM coexpressed both M1 and M2 markers (Figure 2A). Fresh OM express both CD166 (previously shown in Mohamad et al. [2017] and Figure 2A) and Embigin (Figure 2A). FlowSOM (analyzes flow or mass cytometry data using a self-organizing map) analysis (Figure 2B) identified 10 clusters between age-matched OM- and BM-derived macrophages that were completely different from one another except for a very small subpopulation depicted in orange. This color-coded-based cluster designation (Figure 2B) also highlights differences in subgroups contained within OM- and BM-derived macrophages and the heterogeneity of both OM and macrophages when an extensive phenotypic analysis is made. Furthermore, these data show that our isolation protocol yields 2 discrete and distinct groups of CD45$^+$F4/80$^+$ cells.

We investigated whether OM changed with age phenotypically and in numbers. Two examples are shown in Figures 2C and 2D. Therefore, although we examined in this manuscript both neonatal and mature OM, we cannot rule out the possibility that some of the properties of OM may be age or tissue specific. We also examined the origin of OM since macrophages can originate from embryonic progenitors or circulating HSC-derived monocytes (McGrath et al., 2015; Yona et al., 2013). A substantial fraction of recipient OM (5%–30%) survived lethal irradiation 4 months posttransplantation (Figures 2E, S1A, and S1B). Donor Lin$^-$Sca1$^+$c-kit$^+$ (LSK; and competitor cells), however, differentiated into OM (on average, 35%–60%), suggesting that OM are HSC-derived myeloid cells. However, these studies cannot rule out whether a subset of OM is derived embryonically and cannot be replaced by stem cell transplantation.

We compared the expression of OB-associated genes between OM and OB (Figures 2F and 2G) to examine whether OM are genetically related to OB. We examined osteolineage genes because of the description of proximal osteolineage cells (Silberstein et al., 2016) and because we obtained OM by enzymatic digestion of bone, which also yields OB. OM expressed significantly lower levels of mRNA for *Runx2*, *Osterix*, *Collagen1a*, *Osteopontin*, and *Osteocalcin* (Figure 2F). However, OM expressed significantly higher levels of *Embigin*, *Angiogenin*, and interleukin-18 than OB (Figure 2G), suggesting that at the genetic level, OM are similar to HSC proximal osteolineage cells (Silberstein et al., 2016).

To examine the specifics of interactions between OM, OB, and MK to enhance hematopoietic activity (Mohamad et al., 2017); first described in Chitteti et al. (2010a), we tested whether direct contact between MK and OM is essential. Different cell types were placed in transwell dishes as described in the legend of Figure 2. OM failed to expand when OM+OB were physically separated from MK (Figure S1C). Cultures of OM+OB with or without a transmembrane separated MK (upper chamber) were seeded with LSK. In the absence of a transwell, OM+OB maintained their hematopoietic-enhancing activity, which was augmented when MK were added (OM+OB+MK; Figure 2H). However, MK failed to augment colony-forming units (CFU) fold change (Figure 2H), when a membrane separated MK from OM+OB, suggesting that this activity was not mediated by soluble factor(s). Figure 2 summarizes the origin, physical, developmental, and genetic properties of both neonatal and adult OM as we currently know them.

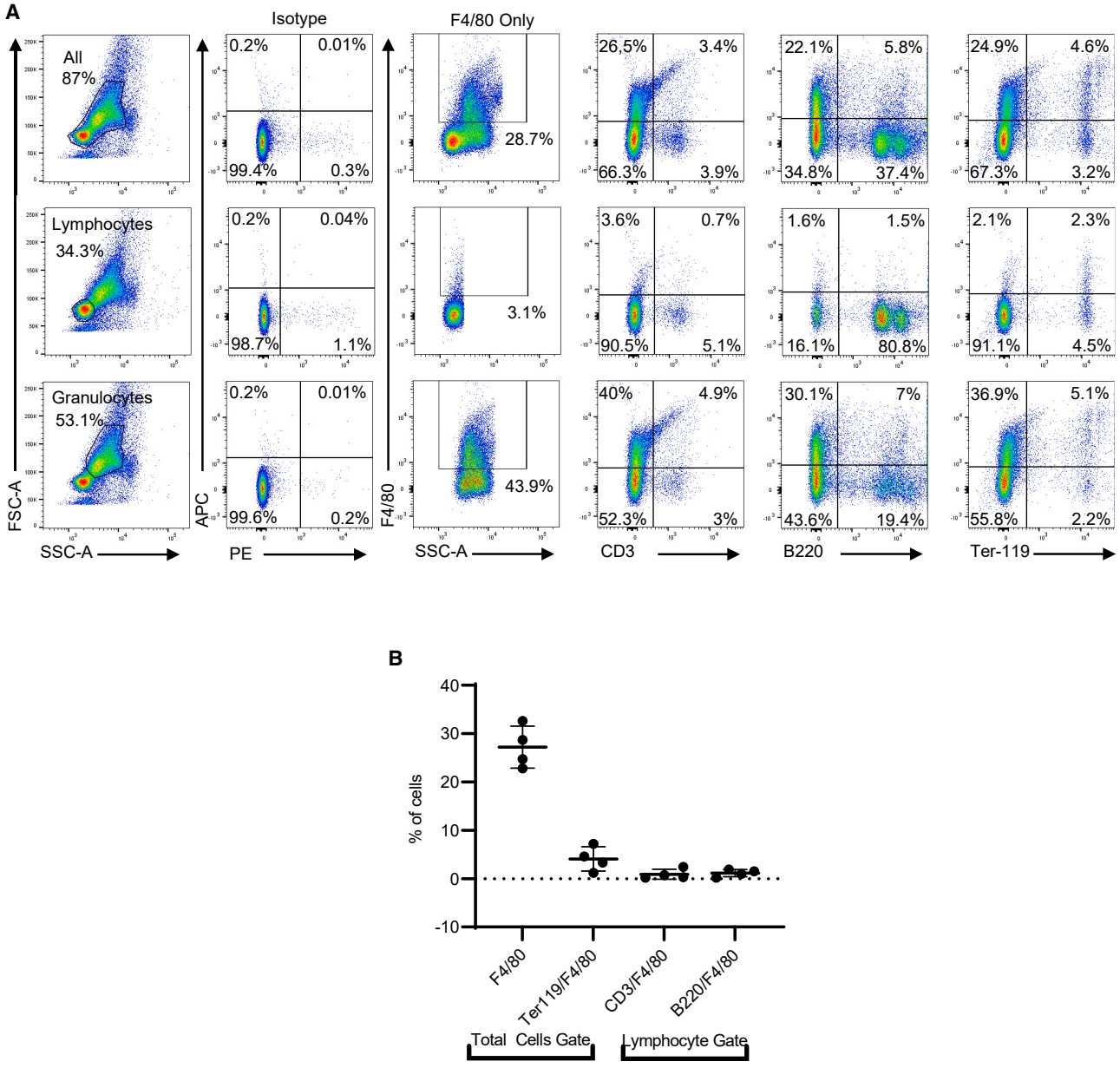

Figure 1. Flow cytometric analysis of BM-derived cells

(A) One of 4 independent experiments dedicated for this analysis. BM cells from 2 to 3 mice per experiment were collected from 8- to 12-week-old mice. BM was flushed aggressively (to facilitate fragmentation) from long bones using a 27G needle and a syringe. Single-cell suspensions were stained with the indicated fluorochrome-conjugated antibodies and analyzed. Cells were gated (across in the 3 rows shown) to contain all of the cells (top row), lymphocytes only (center row), or granulocytes only (bottom row). Backgating of side scatter versus F4/80$^+$ is shown in the third column from the left to reflect the position (relative to side scatter) of F4/80$^+$ cells across the 3 gates used.

(B) Bar graph summarizing data from all 4 experiments dedicated to this analysis. It is important to point out that only 28.7% (26.3% ± 3.7%, in these 4 experiments) of all of the cells were F4/80, unlike the value from Figure 1 in Millard et al., which exceeded 50%. It is critical to note here that fragments from macrophages attached to lymphocytes should have a minimal effect on cell size (forward and side scatter) and no effect whatsoever on granularity (side scatter). Therefore, a discrete population of "contaminated" cells should be observed within the lymphocyte gate. A discrete F4/80$^+$CD3$^+$ or F4/80$^+$B220$^+$ population could not be detected, especially in the lymphocyte gate. Some double staining was detected with Ter-119 that could not be ruled out as nonspecific.

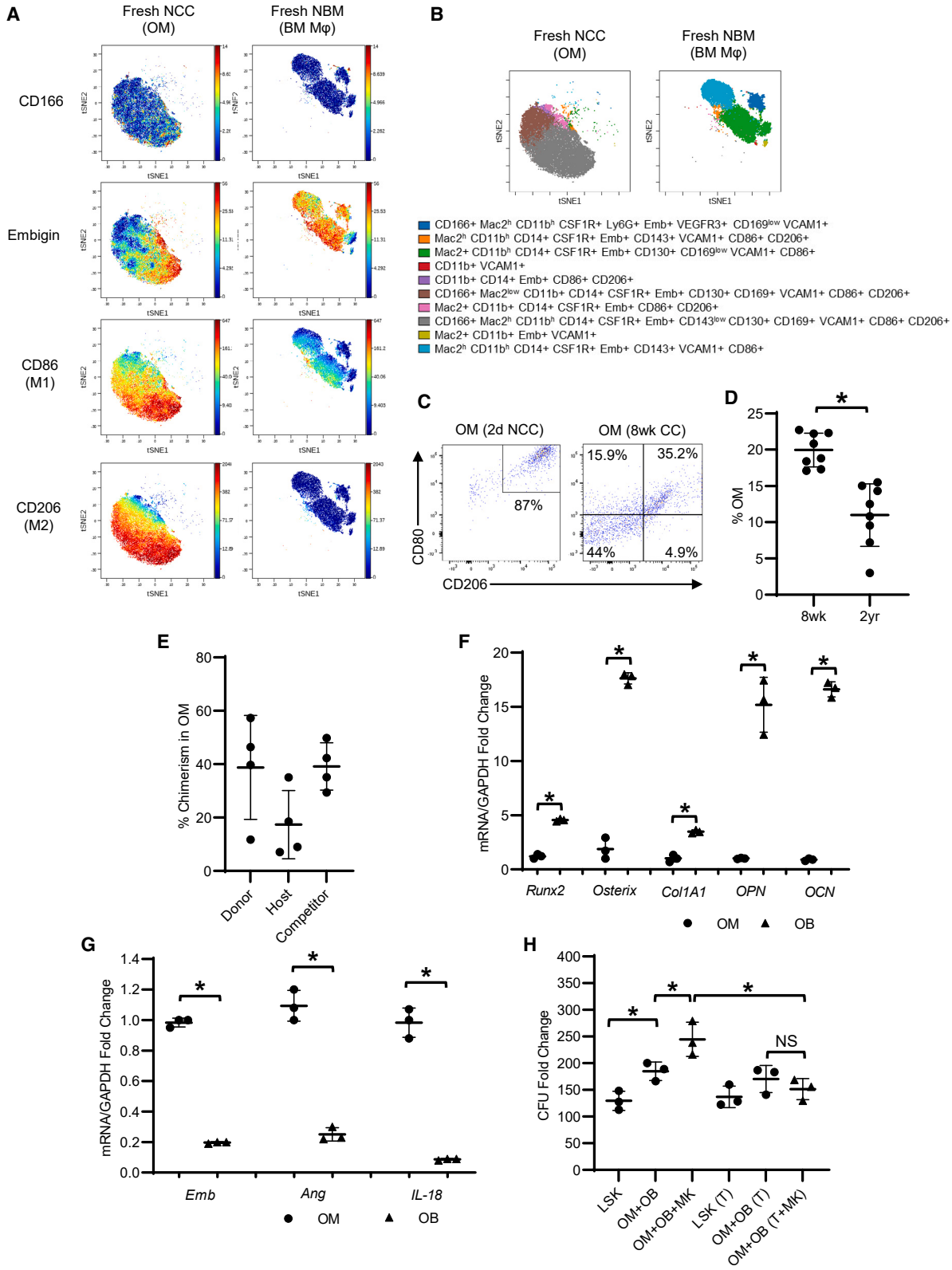

(legend on next page)

Multidimensional single-cell analyses

Single-cell mRNA sequencing (scRNA-seq) was performed to identify mediators through which OM augment hematopoiesis. OM ($CD45^+F4/80^+CD41^-$) from NCC cultured for 16 h with or without MK were subjected to scRNA-seq. A multidimensional scaling plot of the top 2 principal components of significantly expressed genes suggested a difference between OM obtained from NCC and NCC + MK (Figure S1D). A heatmap identified target genes potentially implicated in the augmentation of hematopoiesis (NCC+MK) (Figure 3A). A total of 299 genes (Table S3) were upregulated in OM from NCC+MK compared to those from NCC, whereas 709 genes (Table S4) were downregulated. Several hematopoiesis regulating genes such as *PF-4* (Bruns et al., 2014), *Embigin* (Silberstein et al., 2016), *Fli-1* (Smeets et al., 2013), *Lmo-2* (Zhu et al., 2005), and *Ikzf-1* (Malinge et al., 2013) were upregulated in NCC+MK. scRNA-seq results were validated via qPCR (Figure 3B).

We used liquid chromatography-tandem mass spectrometry (LC-MS/MS) to identify proteins translated from differentially expressed genes. NCC (from CD45.2 mice) were cultured overnight with or without MK. Both groups were cultured for 2 additional days with LSK cells (from CD45.1 mice), after which OM from both cultures ($CD45.2^+CD45.1^-F4/80^+CD41^-$) were sorted and analyzed. The purity of sorted cells always exceeded 95%. Proteins upregulated and downregulated in OM from both groups are listed in Tables S5 and S6, respectively. Embigin was upregulated in OM isolated from NCC+MK compared to other groups as seen in the volcano plots in Figure 3C. There was no difference in Embigin expression levels between OM from cultured and fresh NCC (left plot). Figure 3D shows Embigin abundance in all 3 groups. Thus, Embigin, a protein that was previously implicated in hematopoiesis (Silberstein et al., 2016), was upregulated on OM due to crosstalk between OM, OB, and MK (Figures 3B–3E). OM express Embigin (Figure 2A) constitutively. It is possible that PF4 was upregulated on NCC+MK due to shedding of PF4 by MK in culture. We did not investigate this possibility.

NCC cultured for 2 days with or without MK were also analyzed by single-cell mass cytometry (CyTOF). ViSNE plots (gated on $CD45^+F4/80^+$) and heatmaps were generated to analyze differential protein expression (Figures 3E and 3F). Several surface proteins such as Mac-2 and CD14 were upregulated on OM within NCC+MK cultures compared to OM alone. CD166, an important functional marker of OB and the hematopoietic niche (Cheng et al., 2011; Chitteti et al., 2010a, 2013a, 2014), was upregulated on OM from NCC+MK cultures (Figure 3E). Only CD166 and Embigin were distinctively upregulated on OM from NCC+MK cultures (Figure 3E).

A FlowSOM analysis was performed on ViSNE plots to reveal an unbiased phenotypic heterogeneity between OM contained within both groups. Nine metaclusters were detected for OM contained in NCC and 4 were detected for OM contained in NCC+MK (Figure 3G). Metaclusters 2 and 3 overlapped between the 2 groups. CD166 and Embigin, which were upregulated on OM by interactions with MK (Figure 3E), were detected simultaneously on metaclusters 1, 2, and 5, which increased in size when OM interacted with MK (Figure 3G). Of these, metacluster 1 was unique because it expressed the highest level of Embigin and CD166 and was absent on OM within NCC. Combined,

Figure 2. Characterization of OM

(A and B) Single-cell suspensions of fresh NCC and neonatal BM obtained from the same 2- to 3-day-old pups were analyzed by CyTOF (17 surface antibodies; Table S2). Analysis with these 17 antibodies was repeated 3 times on 3 different samples. Data were gated on singlet viable cells (Ir191/193), event length, and cisplatin (Pt195). The data were gated on $CD45^+F4/80^+$ cells to identify OM in fresh NCC (A, left) and macrophages in NBM (A, right). (A) ViSNE plots indicating differences in individual surface markers between OM and BM macrophages. The collective and relative position of events with respect to one another gated on $CD45^+F4/80^+$ events in the 2 ViSNE plots (tSNE1 vs. tSNE2) indicate that fresh NCC and BM macrophages are phenotypically different with respect to the 17 antibodies used. (B) Heterogeneity within subpopulations of OM and BM macrophages. Each cluster was identified based on the expression of the 17 surface markers. The 10 clusters were negative for the expression of all of the other used markers not indicated in the identity of the clusters; N = 3–6.

(C) Flow cytometric analysis depicting coexpression of CD80 and CD206 on OM in NCC (left dot plot) and 8-week calvarial cells (right dot plot).

(D) Percentage of OM in long bones (relative to total nucleated cells) from 8-week-old and 2-year-old mice, N = 8, Student's t test, $p < 0.05$.

(C) and (D) are shown to highlight developmental changes in phenotype and numbers of OM.

(E) A total of 1,000 LSK from C57BL/6J (CD45.2) mice were transplanted with 2×10^5 BoyJ (CD45.1) cells intravenously (i.v.) in irradiated (900 cGy, 1 dose) F1 recipients. OM were identified by staining for CD45 and F4/80, and their origin was recognized by staining for CD45.1 and CD45.2. Month 4 chimerism is depicted. Additional data are in Figures S1A and S1B.

(F and G) Freshly isolated OM (closed circle) and OB (closed triangle) were analyzed by qPCR for the indicated genes.

(H) Sorted OM and OB were reconstituted at their original NCC percentages and cultured in the absence (OM+OB) or presence (OM+OB+MK) of MK, separated by a 0.4-μm transwell (T) from OM+OB. Cultured cells were assessed for their clonogenic potential on day 7 and CFU fold change determined. N = 3; *$p < 0.05$, 1-way ANOVA. Additional data on the effect of MK contact on the proliferation of OM are shown in Figure S1C.

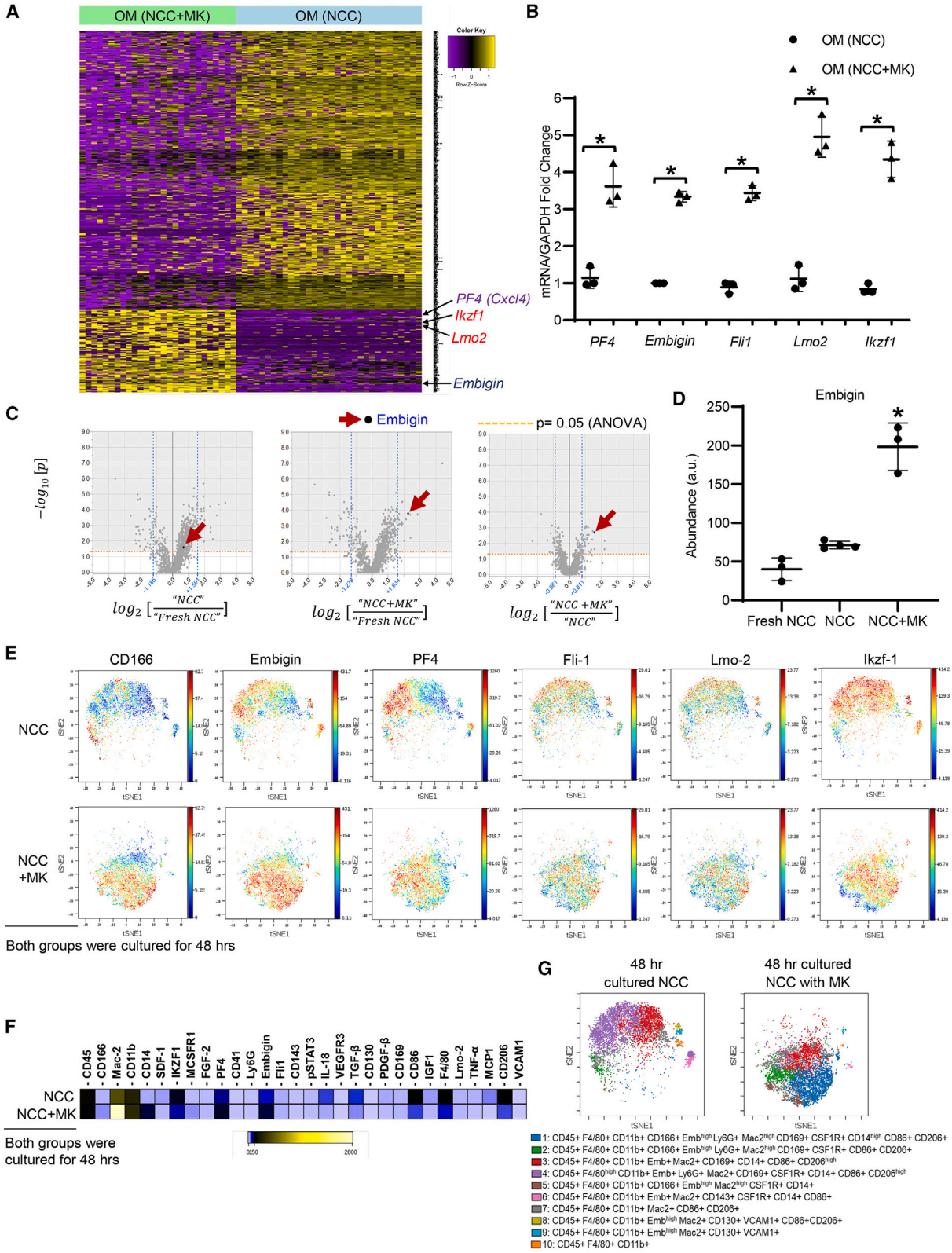

(legend on next page)

these analyses indicate that the expression of CD166 and Embigin on OM is upregulated following the interaction of OM with MK. Furthermore, these results suggest that CD166 and Embigin may act as potential mediators of OM augmentation (via megakaryocyte priming) of the OB-mediated enhancement of hematopoiesis (Chitteti et al., 2010a, 2013a).

CD166 as a molecular mediator of OM function

We previously demonstrated the importance of CD166 expression on NCC in maintaining hematopoiesis (Chitteti et al., 2010a, 2013a, 2014). Sorted $CD166^+$ and $CD166^-$ OM from wild-type (WT) C57Bl/6J NCC (Figure 4A) were cultured with OB from the same NCC preparation ($CD166^+$OM+OB and $CD166^-$OM+OB) and then seeded with LSK. As expected, hematopoietic stem and progenitor cells (HSPC) cocultured with $CD166^-$OM+OB had a significantly lower CFU fold change compared to OM + OB and $CD166^+$OM+OB (Figure 4B), suggesting that $CD166^+$ OM is functionally important in supporting hematopoiesis.

Next, CD166 KO OM ($OM^{CD166-/-}$) or WT OM (OM^{WT}) were cultured with WT OB with or without MK (Figure 4C). $OM^{CD166-/-}$ mice have numbers of OM similar to those of WT mice. Increased CFU fold change was observed in the presence of WT OM and OB, which was further augmented by MK (Figure 4D). $OM^{CD166-/-}$ failed to mediate the same hematopoiesis-enhancing activity (with or without MK), signifying the importance of CD166 in these interactions and suggesting that augmentation of this activity by MK is dependent on the expression of CD166 by OM. Breakdown of CFU subtypes is shown in Figure S1E.

In vitro observations were validated using competitive repopulation assays (Mohamad et al., 2017). LSK maintained with WT OM+OB+MK sustained the highest level of chimerism in primary recipients (Figure 4E). However, substituting WT OM with $OM^{CD166-/-}$ caused a significant decline in the hematopoietic-enhancing activity (Figure 4E), suggesting that CD166 is an important OM mediator involved in maintaining hematopoiesis. BM data 4 months post-transplant are shown in Figure 4F. Multilineage reconstitution in primary recipients is shown in Figure 4G.

Embigin and OM function

To examine the impact of Embigin in the niche, an anti-*Embigin* blocking antibody was used. Progenitor assays demonstrated a decline in CFU fold change activity compared to controls (Figure 5A), indicating that blocking Embigin on OM and OB negatively affects hematopoietic activity. We also used a short hairpin RNA (shRNA)-mediated *Embigin* knockdown (Figure 5B). NCC were infected (*Embigin* shRNAs lentiviruses or empty virus) and then cultured with MK for 7 days, after which shRNA knocked down OM, and empty virus OM, uninfected OM, and uninfected OB were sorted (gating strategy in Figure S2A). These fractions were cultured with OB and seeded with LSK (Figure 5C). No significant difference was observed in CFU fold change in cultures of uninfected OM and OB (labeled as OM+OB+MK) and empty virus-infected OM and OB (OM^{EV}+OB+MK). However, CFU fold change declined when *Embigin* KD (knockdown) OM ($OM^{Emb\ KD}$) were used (Figure 5C; observed with 2 shRNA constructs). These data indicate that the loss of megakaryocyte-induced augmentation of Embigin expression on OM affects the ability of these cells to augment the enhancement of hematopoietic function (Chitteti et al., 2010a). Clonogenic distribution of progenitors is shown in Figure S2B.

The results in Figure 5C were validated *in vivo* (Figures 5D and S3A). LSK maintained with OM^{EV}+OB+MK repopulated recipients significantly higher than LSK maintained with $OM^{Emb\ KD}$+OB+MK. Interestingly, multilineage

Figure 3. OM, OB, and MK interactions

(A) NCC from 2- to 3-day-old pups were cultured for 16 h in the absence (NCC) or presence of MK (NCC+MK). OM ($CD45^+F4/80^+CD41^-$) were sorted from the 2 groups and subjected to single-cell capture. A total of 24 OM from NCC and 20 from NCC+MK underwent single-cell mRNA sequencing.

(B) qPCR of target genes in (A) to validate single-cell mRNA sequencing. N = 3; *p < 0.05; 1-way ANOVA.

(C and D) NCC were cocultured overnight in the absence (NCC) or presence (NCC+MK) of MK. Each group was seeded with LSK for 2 days, followed by OM isolation via cell sorting. OM from each group were subjected to TMT-based peptide labeling and LC-MS/MS. OM isolated from fresh NCC and not cultured served as controls. A total of 1,548 proteins were identified and 1,359 proteins were quantified. (C) Volcano plots comparing protein expression of OM within NCC and fresh NCC (left), NCC+MK and fresh NCC (center), and NCC+MK and NCC (right). The highlighted dot in black (red arrow) is the expression level of Embigin in all 3 plots. The orange dotted line is the 0.05 p value cutoff. (D) Average grouped abundance of Embigin in all 3 groups. Statistical accuracy was estimated using SE. N = 3–4.

(E–G) Single-cell suspensions of NCC were cultured for 2 days with or without MK and analyzed using a panel of 30 surface and intracellular antibodies (Table S1; each antibody was titrated to determine optimal concentration). Raw data were gated on singlet viable cells, event length, and cisplatin as described in Figure 2. Data were gated on $CD41^-CD45^+F4/80^+$ cells to identify OM in NCC and NCC cultured with MK. (E) ViSNE plots of OM obtained from NCC and NCC+MK showing the expression of some markers, including CD166 and Embigin. (F) Heatmap demonstrating the expression of 30 antibodies on OM obtained from NCC and NCC+MK. N = 3. (G) Representation of the heterogeneity observed within subpopulations of OM from NCC and NCC+MK. Each subpopulation was characterized depending on their expression of 17 surface markers.

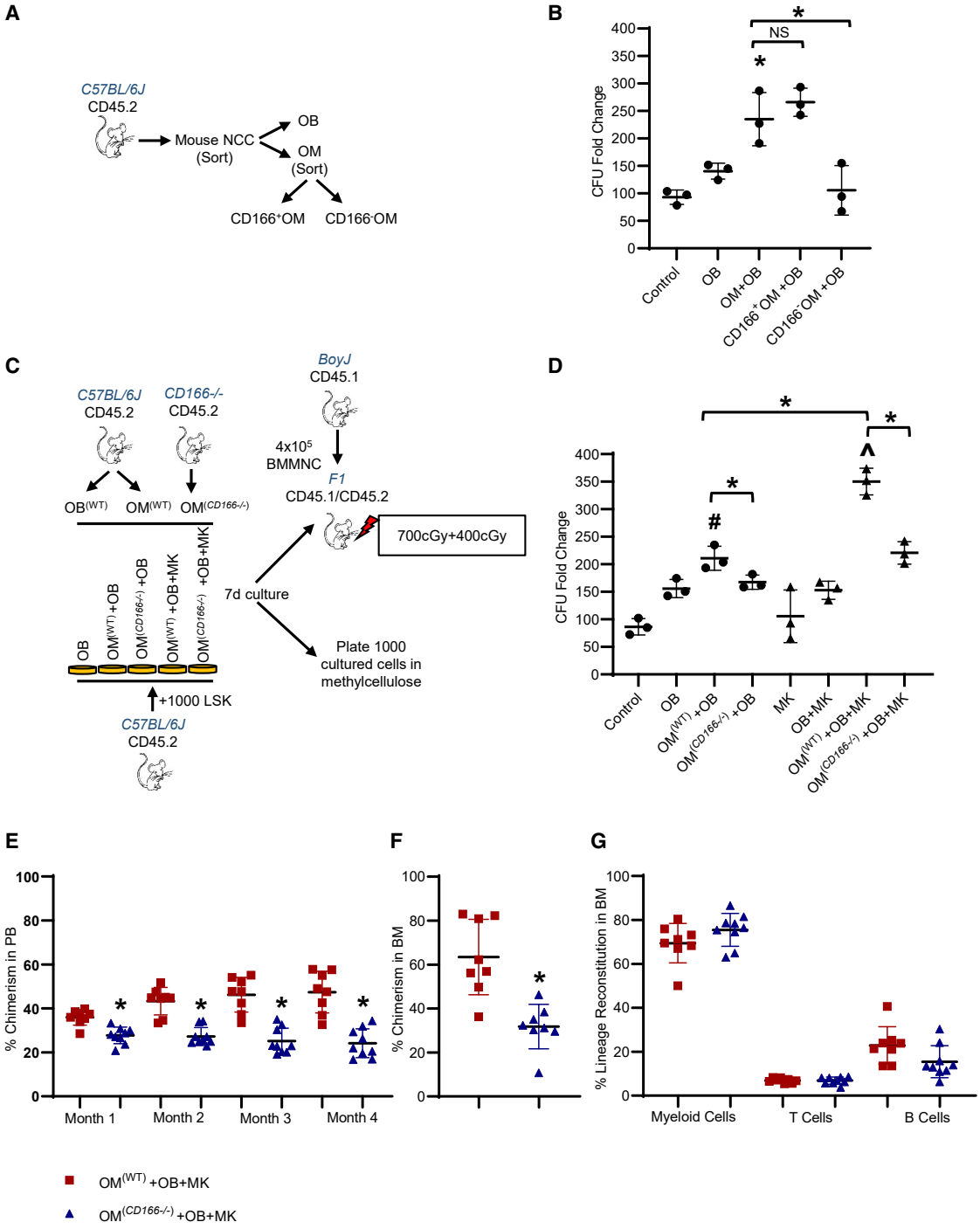

Figure 4. Effects of CD166 expression on OM on the hematopoietic function

(A) Schematic representation of NCC flow cytometry fractionation (from 2- to 3-day-old pups).

(B) $CD166^+$ and $CD166^-$ OM were isolated by cell sorting and plated with OB ($CD45^-F4/80^-$ cells from NCC) and then seeded with LSK for 7 days. CFU assays were established to determine CFU fold change of cultured LSK progeny. One of 3 independent experiments performed in triplicate; *p < 0.05 vs. all controls besides $CD166^+$OM+OB; 1-way ANOVA.

(C) Experimental design for the progenitor (D) and competitive repopulation assay (E–G). Cell viability in all cultures exceeded 97%. We previously demonstrated (Cheng et al., 2011; Chitteti et al., 2010b, 2013b) that in these cultures, only LSK progeny display any CFU function or engraftment potential. Cocultures of NCC-derived OB were mixed with either the original number of OM contained in freshly

(legend continued on next page)

reconstitution in primary recipients demonstrated a lymphoid bias in LSK maintained with $OM^{Emb\ KD}$+OB+MK (Figures 3SA and S3B). Since Embigin is a cell adhesion molecule (Huang et al., 1993) associated with homing (Silberstein et al., 2016), we assessed the homing of donor LSK to the BM. There was no difference in the number or percent recovery of LSK progeny cultured with OM^{EV}+OB+MK and $OM^{Emb\ KD}$+OB+MK (Figure S3C) or the ability of transplanted/homed cells to proliferate (Figure S3D). Interestingly, WT LSK cells engrafted to the same level in WT and global *Embigin* KO mice (data not shown).

Recombinant CD166 and Embigin partially substitute OM function

Progenitor assays were performed to determine whether recombinant CD166 (rCD166) and Embigin (rEmb) could substitute for OM activity *in vitro*. BSA (control), rCD166, and rEmb were coated onto tissue culture plates (Zhang et al., 2019), which were used to culture OB (from NCC). No significant differences in CFU fold change were observed between OM+OB, rCD166+OB, rEmb+OB, and rCD166+rEmb+OB, indicating that rCD166 and rEmb could partially substitute for OM-mediated enhancement of hematopoietic activity (Figure 5E). As expected, CFU fold change was significantly higher compared to OB cultured on BSA. In all of the experiments (N = 3), the same nonsignificant trend was observed in which rCD166+rEmb+OB was slightly upregulated compared to rCD166+OB and rEmb+OB, suggesting that the effect of the combination of recombinant proteins may be additive, rather than synergistic (Figure 5E). CFU breakdown is shown in Figure S4. Interestingly, knocking down Embigin on $OM^{CD166-/-}$ (double KD) did not further decline OB-mediated hematopoietic activity, confirming the additive rather than the synergistic effects of these molecules. These data demonstrate that CD166 and Embigin partially substitute for OM-mediated enhancement of hematopoietic activity.

DISCUSSION

Here, we documented that OM are a distinctive population of the hematopoietic niche, that OM- and BM-derived macrophages share common features but are distinct cells, and that OM and BM-derived macrophages can be effectively separated from one another. We also demonstrated that we can purify macrophages and OM from flushed BM and digested bones, respectively, demonstrating that at least in our hands, the fragmentation of macrophages that Millard et al. described does not happen. Our previous (Mohamad et al., 2017) and present data demonstrate that differences between OM- and BM-derived macrophages are phenotypic, functional, and molecular. We illustrated that direct contact between OM, OB, and MK is critical for augmentation of the hematopoietic activity (Figures 2H and S1C), suggesting that this activity is probably not communicated through soluble factor(s). It is critical to emphasize that OM, OB, and MK are present in the BM of neonatal as well as adult mice and have been previously implicated in hematopoiesis and the maintenance of HSC function. It is important to stress here that we used neonatal calvariae as a source of OM in most of our studies because this tissue yielded the highest number of OM and is the easiest source from which to collect OM.

The importance of OB in regulating the hematopoietic niche is well established (Calvi et al., 2003; Cheng et al., 2011; Chitteti et al., 2010b; Zhang et al., 2003). However, not much is known about interactions between OB and other niche cells such as OM and MK and how together they regulate hematopoiesis. Although OM are residents of the hematopoietic niche, more is known about their function in bone modeling (Alexander et al., 2011; Batoon et al., 2017, 2019; Chang et al., 2008; Cho et al., 2014; Chow et al., 2013) than in hematopoiesis. Winkler et al. (2010) established that loss of OM caused a concurrent disruption of the endosteal niche and mobilization of HSPC from the BM to the blood. We recently established the importance of crosstalk between OM, OB, and MK to regulate hematopoietic function (Mohamad et al., 2017). Here, we focused our efforts on determining potential mediators that are triggered by crosstalk among those cell types and examined whether these mediators participate in supporting this activity.

Single-cell studies identified Embigin and CD166 on OM as potential targets that are amplified following NCC-MK interactions (Figures 3C–3E). It is important to stress that freshly isolated OM express CD166 (Mohamad et al.,

isolated NCC (OM^{WT}+OB) or a complementary number (equivalent to the original number of OM in NCC) of CD166 KO OM ($OM^{CD166-/-}$+OB) in the absence or presence of MK. Overnight cultures were seeded with LSK and cultured for 1 more week with each of the groups mentioned above.

(D) Cultures were used to determine CFU fold change of LSK progeny. One of 3 independent experiments performed in triplicate. $^{\#}p < 0.05$ vs. controls without MK, $^{\wedge}p < 0.05$ vs. controls with MK, $^{*}p < 0.05$; 1-way ANOVA.

(E–G) Recipients (F1 mice) were irradiated (split-dose of 700 and 400 cGy, 4 h apart) and received i.v. test cells (1,000 freshly isolated LSK cells or their cultured progeny) in 200 μL PBS. Cells were transplanted in a competitive repopulation assay with 400,000 BoyJ (CD45.1) cells. (E) Monthly data were analyzed via peripheral blood chimerism. (F) Chimerism observed in BM at 4 months posttransplant (G) Multilineage reconstitution in month 4 BM. N = 5–9 mice/group; $^{*}p < 0.05$; 1-way ANOVA.

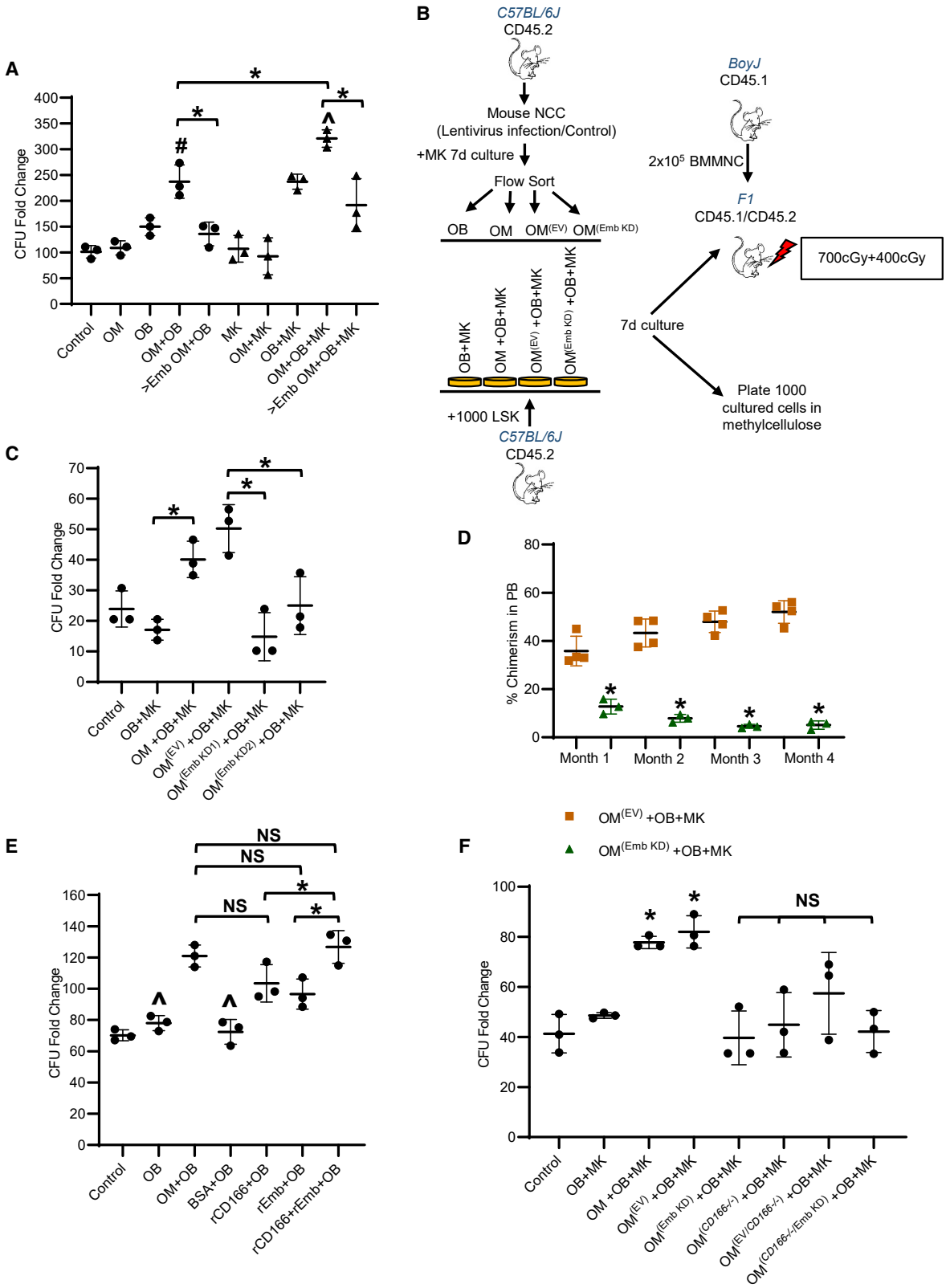

(legend on next page)

2017) and Embigin (Figures 2A and 3E). Through undetermined mechanisms, interaction with MK causes an upregulation of these 2 molecules, which in turn, increase the ability of OM to augment the OB-derived enhancement of hematopoietic function (Chitteti et al., 2010b). Interfering with CD166 or Embigin on OM partially abrogated their ability to augment the enhancing activity of OB. Embigin, a molecule implicated in hematopoiesis (Silberstein et al., 2016), was upregulated at the mRNA, as well as the translational levels. Embigin was one of the 7 top targets in MS data (Figures 2C; Table S5). Conversely, CD166, which is a critical molecule for HSC and the hematopoietic niche (Cheng et al., 2011; Chitteti et al., 2010a, 2013a, 2014) was not upregulated on OM at the single-cell mRNA level following the crosstalk between OM, OB, and MK. Also, CD166 was not a candidate protein in the MS data. However, the CyTOF data demonstrated an upregulation of CD166 (Figure 3E), indicating possible regulation at the translational level. The reason for this discrepancy between different assays is not known at this point.

Do CD166 and Embigin mediate the observed OM augmentation of the hematopoiesis-enhancing activity of osteoblasts? Previous investigations established that proximal osteolineage cells express Embigin and are involved in the maintenance of hematopoiesis (Silberstein et al., 2016). Here, our *in vitro* and *in vivo* functional assays illustrated the importance of Embigin as a regulator of OM-mediated hematopoietic function (Figure 5) and further implicated Embigin in sustaining hematopoiesis. However, using global Embigin KO mice as recipients, we could not demonstrate the loss of engraftment of WT stem cells (data not shown). This may explain why the effect of Embigin on transplantation was only evident when we previously used blocking antibodies (Silberstein et al., 2016). In the present study, both antibody-based and shRNA KD studies were used to determine the effects of loss of Embigin expression on OM. Both approaches demonstrated that a decline in Embigin expression was detrimental to the ability of OM to augment hematopoiesis. It is possible that the impact of Embigin on engraftment can be observed only after serial transplantation in *Embigin* KO mice. Studies with recombinant proteins demonstrated that Embigin and CD166 are mediators that can partially substitute for OM and augment the OB-mediated hematopoiesis-enhancing activity *in vitro* (Figures 5E and 5F). In this setting, recombinant proteins fell short of enhancing hematopoiesis to the level observed with NCC+MK. The reasons behind this are plentiful, including the use of a 2-dimensional (2D) assay system, the possible nonphysiologic concentrations of Embigin and CD166 alone or relative to one another, and, most likely, the contribution of other mediators that were not examined.

CD166 studies were more expansive due to prior laboratory experience and availability of CD166 KO mice (Cheng et al., 2011; Chitteti et al., 2010a, 2014; Xu et al., 2016). We previously demonstrated in multiple settings the importance of CD166 in maintaining HSC and progenitor cell function and the competence of the hematopoietic niche (Cheng et al., 2011; Chitteti et al., 2010a, 2014; Zhang et al., 2019). Here, we demonstrated that OM function is also dependent on CD166 expression. The importance of

Figure 5. Effcets of Embigin expression on OM on hematopoietic function

(A) OM and OB cultures in the absence or presence of MK. An Embigin blocking antibody (>Emb; 1 μg/well) was added on days 0, 3, and 6 of culture. On day 7, excess antibody was washed away, and LSK were added to cultures. This approach blocked Embigin temporarily on OM, OB, and MK, but not on LSK. One of 3 independent experiments performed in triplicate. Cell viability in all of the cultures exceeded 97%. We have previously shown (Cheng et al., 2011; Chitteti et al., 2010b, 2013b) that in these cultures, only LSK progeny displayed any CFU function or engraftment potential. $^{\#}p < 0.05$ vs. all controls without MK; $\hat{}p < 0.05$ vs. all controls with MK; 1-way ANOVA.

(B) Schematic representation of the progenitor (C) and competitive repopulation assay (D). NCC were subjected to 4 spinfections with shRNA or an empty vector over 2 days. After the fourth spinfection, MK were added for 1 week. On day 7, $GFP^{+}Emb^{-}$ OM (labeled as $OM^{(Emb\ KD)}$) and GFP+Emb+OM (labeled as $OM^{(EV)}$) were sorted. Overnight cocultures were set up with virus-infected OM and uninfected OB. Uninfected OM+OB+MK served as control. LSK were then cultured for 1 week with each group.

(C) Progenitor assays were set up to determine CFU fold change. CFU decline was observed with 2 shRNA constructs ($OM^{Emb\ KD1}$+OB+MK and $OM^{Emb\ KD2}$+OB+MK). One of 3 independent experiments performed in triplicate. $*p < 0.05$; 1-way ANOVA.

(D) LSK progeny were transplanted i.v. in a competitive repopulation assay with 200,000 BoyJ (CD45.1) cells in irradiated (700 and 400 cGy, split-dose) F1 recipients. Monthly data were analyzed via peripheral blood chimerism.

(E) Recombinant murine CD166 and Embigin (as a substitute for OM) were coated on tissue culture plates. These plates were used to culture OB sorted from NCC. Cultures were seeded with LSK to determine CFU fold change. One of 3 independent experiments performed in triplicate. $*p < 0.05$, $\hat{}p < 0.05$ vs. OM+OB, rCD166+OB, rEmb+OB and rCD166+rEmb+OB; 1-way ANOVA.

(F) CD166 KO NCC were subjected to 4 spinfections over a span of 2 days to infect them with GFP^{+} virus containing shRNA against *Embigin* or an empty vector. At the end of the fourth spinfection, MK were cultured for 1 week with each of these groups. On day 7, these cultures were used to flow cytometrically sort for OM, which were $GFP^{+}Emb^{-}$ or $GFP^{+}Emb^{+}$. Overnight cocultures were set up with virus-infected OM and uninfected OB. LSK were cultured for 1 week with each of these groups. Progenitor assays were set up to determine CFU fold change of cultured LSK progeny relative to 250 fresh LSK. One of 3 independent experiments performed in triplicate. $*p < 0.05$ vs. LSK, OB, $OM^{(Emb\ KD)}$+OB + MK, $OM^{(CD166-/-)}$ +OB+MK, $OM^{(EV/CD166-/-)}$+OB+MK, $OM^{(CD166-/-/Emb\ KD)}$+OB+MK; 1-way ANOVA.

CD166 expression on OM function was established via the sorting from WT mice CD166$^-$ and CD166$^+$ OM. CD166 expression on OM was upregulated due to the crosstalk between OM, OB, and MK. The absence of CD166 affected hematopoietic activity, which was maximal when LSK cocultured with WT OM, OB, and MK were transplanted (Figures 4E and 4F). How MK induce the upregulation of CD166 and Embigin on OM remains to be determined.

Overall, our work identifies OM as a critical cell within the hematopoietic niche that is functionally different from BM-derived macrophages and establishes CD166 and Embigin as novel modulators of stem cell function. These studies also confirm the role of MK in sustaining HSC activity through a supportive function targeted at OB and OM. From a practical point of view, these studies promote similar investigations in which recombinant proteins (e.g., CD166, Embigin) can be used to manipulate HSC *in vitro* for a short period of time without an appreciable loss of engraftment and repopulation potentials. Interestingly, these studies can also contribute to the construction of 3D systems in which multiple soluble factors and defined cellular elements of the niche are combined (simultaneously or sequentially) to create a more physiologic *in vitro* system for HSC maintenance.

EXPERIMENTAL PROCEDURES

Resource availability

Lead contact

Edward F. Srour

Materials availability

Please contact the corresponding author for the same.

Data and code availability

- The scRNA-seq data discussed in this publication have been deposited in the GEO: GSE254995 (Edgar et al., 2002) (https://www.ncbi.nlm.nih.gov/geo/query/acc.cgi?acc=GSE254995).
- Raw and processed mass spectrometry data have been uploaded to the MassIVE repository, a ProteomeXchange partner, with accession number MSV000093840 (https://doi.org/10.25345/C5Z02ZK81).

Mice

BoyJ, C57BL/6J, C57BL/6XBoyJ F1, CD166, and Embign KO mice (8–12 weeks old) were bred and housed at Indiana University School of Medicine (IUSM). Animal protocols were approved by the Institutional Animal Care and Use Committee of the IUSM and followed NIH guidelines.

OM from fresh NCC and long adult bones

NCC were prepared from 2- to 3-day-old neonatal pups (Ghosh et al., 2019; Kacena et al., 2012). Calvariae were pretreated with 4 mM EDTA in PBS for 30 min followed by sequential collagenase digestions (Worthington Type 2 [catalog no. CLS-2] at 200 U/mL for 15 min/round). Cells collected in the first and second rounds of digestion with collagenase were discarded. Cells from rounds 3–5 were collected as previously described (Ghosh et al., 2019; Kacena et al., 2012). These were labeled NCC and were >95% CD45$^-$cells and ∼5% OM (CD45$^+$F4/80$^+$), as previously demonstrated (Mohamad et al., 2021). Whenever head-to-head comparisons were made between OM- and BM-derived macrophages, crushed long bones from age-matched donors (2- to 3-day-old neonatal pups) were used to isolate BM-derived macrophages. Adult bones (8- to 12-week-old mice) were gently flushed to collect BM cells and ultimately BM-derived macrophages (CD45$^+$F4/80$^+$ cells). Flushed bones were crushed lightly and washed with PBS, which was discarded, and then digested sequentially with collagenase (Worthington Type 2 at 200 U/mL for 15 min). Fraction 1 was discarded, and fractions 2–4 were collected then sorted to obtain CD45$^+$F4/80$^+$ OM (Mohamad et al., 2017). We used NCC as a source of OM in most of our studies because this tissue is devoid of BM and is the easiest source to collect OM.

Fetal liver-derived MK

Fetal (embryonic days [E]13–15) liver cells (Kacena et al., 2004, 2012) were seeded in 10 cm^2 culture dishes, in DMEM, 10% fetal calf serum containing 1% thrombopoietin. MK were obtained 3–5 days later using an albumin gradient.

Flow cytometry

Cells were stained with CD45 and F4/80 (BioLegend) and sorted (SORP, FACSAria, or FacsFusion) into CD45$^+$F4/80$^+$ defined as OM and CD45$^-$F4/80$^-$ defined as OB. BM cells were stained with phycoerythrin-conjugated lineage anti-mouse CD3, CD4, CD45R, Ter-119, and Gr1 (BioLegend); APC c-Kit (BioLegend), and FITC Sca-1 (BioLegend) and sorted for LSK cells as described by Chitteti et al. (2010a, 2014). Anti-CD166 and anti-Embigin were obtained from eBiosciences. The purity of sorted cells exceeded 95%. Clones of antibodies used in this study are listed in Table S1.

scRNA-seq

A total of 1 × 10^5 NCC were cultured for 16 h with or without 50,000 MK were stained with CD45, F4/80, and CD41. Sorted CD45$^+$F4/80$^+$CD41$^-$ cells (OM) were suspended at 3 × 10^5 cells/mL PBS and then dispensed into medium-sized integrated fluidic circuit chips (Fluidigm C1 Single-Cell Auto Prep System) (Zhang et al., 2019). mRNA was isolated followed by cDNA synthesis (Clontech SMART-Se version 4 Ultra Low Input RNA Kit). Up to 0.4 ng cDNA was used for library preparation and indexing with Nextera XT DNA Library Prep Kit (Illumina). A total of 24 OM sorted from cultured NCC and 20 OM sorted from cultured NCC+MK were used for library construction. Pooled libraries (4 nM, quality checked) were used for 150 paired-end sequencing (NextSeq 500). Cells that passed quality testing were analyzed. Cluster analysis was conducted using Seurat with default parameters (25867923). Differential gene expression analysis was conducted by an in-house method—left truncated mixture Gaussian-differential gene expression (Wan et al., 2019) — with $p < 0.001$ as the significance cutoff.

CyTOF

Cells were treated with 10 μg/mL Brefeldin A (Sigma-Aldrich) for 3 h, resuspended in PBS, and then stained with Cell-ID Cisplatin (DVS Sciences, Fluidigm). Cells were washed (0.1% BSA, 0.1% Na-azide, and 10 nM EDTA) and blocked (Fc-Receptor; BioLegend), stained for extracellular markers (4°C for 30 min), washed, and fixed (1.5% formaldehyde for 30 min), followed by 2 washes with Maxpar Perm-S Buffer (DVS Sciences, Fluidigm). Cells were stained with intracellular antibodies (30 min), washed, and incubated overnight in 1:1,000 Cell-ID Intercalator-Ir. Samples were resuspended in 1× EQ calibration beads (DVS Sciences) and acquired on a CyTOF2 mass cytometer (DVS Sciences). Antibody details are in the supplemental information.

MS

Mass tag (TMT)-based peptide labeling and LC-MS/MS were used (IUSM Proteomics Core Facility as described; Mosley et al., 2009; Watkins et al., 2018). RAW files were analyzed using Proteome Discover 2.2 (Thermo Fisher). The FASTA database used was a mouse proteome from Uniprot. Percolator false discovery rate was set at 0.01 and 0.05 for strict and relaxed settings, respectively.

Cell cultures

Cultures were maintained in a 1:1 mix of IMDM and α-MEM supplemented as previously described by Chitteti et al. (2010a) and in the figure legends. For *Embigin* KD, an shRNA targeting the 3′ UTR region CCGGGCACAGAAGTAGCTTTATGAACTCGAGTTCATA AAGCTACTTCTGTGCTTTTTG and another targeting the coding region CCGGCGGGTGACTTCAATACAACTACTCGAGTAGTTG TATTGAAGTCACCCGTTTTTG were subcloned in pLKO.1-CMV-tGFP lentivector to generate high-titer stocks. Stocks were used for sequential spinfections, as previously described (Layer et al., 2020).

Clonogenic assays and transplantation studies

Cells were seeded in triplicate in 1.0 mL Methocult (GF M3434, StemCell Technologies). Colonies were scored on day 7. For transplantation, 8- to 12-week-old F1 mice were irradiated (700 and 400 cGy 4 h apart) and transplanted (Chitteti et al., 2010a) with 1,000 LSK cells plus 2 × 10^5 competitor BoyJ (CD45.1) cells or the progeny of 1,000 LSK cells cultured for 7 days under various conditions (see the figure legends). Chimerism was assessed monthly for 4 months. At 4 months, 500,000 BM cells from primary recipients were transplanted into a lethally irradiated secondary recipient. Freshly isolated or cultured NCC do not contain any measurable clonogenic or reconstituting cells (Chitteti et al., 2010a).

Statistical analysis

Data are presented as mean ± SD. All of the experiments (except single-cell genomics and some competitive repopulating assays) were repeated a minimum of 3 independent times in triplicate in each experiment. The results from 1 representative experiment are shown with the corresponding statistical analyses, with the results of all of the other experiments in full agreement. Independent experiments are presented to avoid interexperimental variation, which precludes the pooling of data. Statistical differences were determined using 1-way ANOVA, followed by a Tukey-Kramer post hoc analysis. Significance was set at $p < 0.05$.

SUPPLEMENTAL INFORMATION

Supplemental information can be found online at https://doi.org/10.1016/j.stemcr.2024.02.004.

ACKNOWLEDGMENTS

We thank Indiana University Melvin and Bren Simon Cancer Center Flow Cytometry Resource Facility (FCRF) for their outstanding technical support. We acknowledge the *In Vivo* Therapeutics Core (IVC). FCRF and the IVC are partially funded by NCI grant P30 CA082709 and National Institute of Diabetes and Digestive and Kidney Diseases (NIDDK) grant U54 DK106846 (to E.F.S.). FCRF is partially supported by the NIH instrumentation grant 1S10D012270 (to E.F.S.). This work was supported by NIDDK grant R01 DK118782 (to E.F.S.) and was also partially supported by NIAMS grant R01 AR060332 (to M.A.K.).

AUTHOR CONTRIBUTIONS

S.F.M., R.E.K., J.G., R.B., A.G., and J.L. designed and performed the research. S.F.M. and J.G. analyzed the data and wrote the paper. C.Z. analyzed the data. U.D. analyzed the data and edited the manuscript. M.A.K. and E.F.S. designed the research, analyzed the data, and wrote the paper. E.F.S. conceived and supervised the study.

DECLARATION OF INTERESTS

The authors declare no competing interests.

Received: August 24, 2022
Revised: February 6, 2024
Accepted: February 7, 2024
Published: March 7, 2024

REFERENCES

Alexander, K.A., Chang, M.K., Maylin, E.R., Kohler, T., Müller, R., Wu, A.C., Van Rooijen, N., Sweet, M.J., Hume, D.A., Raggatt, L.J., and Pettit, A.R. (2011). Osteal macrophages promote in vivo intramembranous bone healing in a mouse tibial injury model. J. Bone Miner. Res. *26*, 1517–1532. https://doi.org/10.1002/jbmr.354.

Batoon, L., Millard, S.M., Raggatt, L.J., and Pettit, A.R. (2017). Osteomacs and Bone Regeneration. Curr. Osteoporos. Rep. *15*, 385–395. https://doi.org/10.1007/s11914-017-0384-x.

Batoon, L., Millard, S.M., Wullschleger, M.E., Preda, C., Wu, A.C.K., Kaur, S., Tseng, H.W., Hume, D.A., Levesque, J.P., Raggatt, L.J., and Pettit, A.R. (2019). CD169(+) macrophages are critical for osteoblast maintenance and promote intramembranous and endochondral ossification during bone repair. Biomaterials *196*, 51–66. https://doi.org/10.1016/j.biomaterials.2017.10.033.

Bruns, I., Lucas, D., Pinho, S., Ahmed, J., Lambert, M.P., Kunisaki, Y., Scheiermann, C., Schiff, L., Poncz, M., Bergman, A., and Frenette, P.S. (2014). Megakaryocytes regulate hematopoietic stem

cell quiescence through CXCL4 secretion. Nat. Med. *20*, 1315–1320. https://doi.org/10.1038/nm.3707.

Calvi, L.M., Adams, G.B., Weibrecht, K.W., Weber, J.M., Olson, D.P., Knight, M.C., Martin, R.P., Schipani, E., Divieti, P., Bringhurst, F.R., et al. (2003). Osteoblastic cells regulate the haematopoietic stem cell niche. Nature *425*, 841–846. https://doi.org/10.1038/nature02040.

Chang, M.K., Raggatt, L.J., Alexander, K.A., Kuliwaba, J.S., Fazzalari, N.L., Schroder, K., Maylin, E.R., Ripoll, V.M., Hume, D.A., and Pettit, A.R. (2008). Osteal tissue macrophages are intercalated throughout human and mouse bone lining tissues and regulate osteoblast function in vitro and in vivo. J. Immunol. *181*, 1232–1244.

Cheng, Y.H., Chitteti, B.R., Streicher, D.A., Morgan, J.A., Rodriguez-Rodriguez, S., Carlesso, N., Srour, E.F., and Kacena, M.A. (2011). Impact of maturational status on the ability of osteoblasts to enhance the hematopoietic function of stem and progenitor cells. J. Bone Miner. Res. *26*, 1111–1121. https://doi.org/10.1002/jbmr.302.

Chitteti, B.R., Bethel, M., Kacena, M.A., and Srour, E.F. (2013a). CD166 and regulation of hematopoiesis. Curr. Opin. Hematol. *20*, 273–280.

Chitteti, B.R., Bethel, M., Voytik-Harbin, S.L., Kacena, M.A., and Srour, E.F. (2013b). In vitro construction of 2D and 3D simulations of the murine hematopoietic niche. Methods Mol. Biol. *1035*, 43–56. https://doi.org/10.1007/978-1-62703-508-8_5.

Chitteti, B.R., Cheng, Y.H., Poteat, B., Rodriguez-Rodriguez, S., Goebel, W.S., Carlesso, N., Kacena, M.A., and Srour, E.F. (2010a). Impact of interactions of cellular components of the bone marrow microenvironment on hematopoietic stem and progenitor cell function. Blood *115*, 3239–3248. https://doi.org/10.1182/blood-2009-09-246173.

Chitteti, B.R., Cheng, Y.H., Streicher, D.A., Rodriguez-Rodriguez, S., Carlesso, N., Srour, E.F., and Kacena, M.A. (2010b). Osteoblast lineage cells expressing high levels of Runx2 enhance hematopoietic progenitor cell proliferation and function. J. Cell. Biochem. *111*, 284–294. https://doi.org/10.1002/jcb.22694.

Chitteti, B.R., Kobayashi, M., Cheng, Y., Zhang, H., Poteat, B.A., Broxmeyer, H.E., Pelus, L.M., Hanenberg, H., Zollman, A., Kamocka, M.M., et al. (2014). CD166 regulates human and murine hematopoietic stem cells and the hematopoietic niche. Blood *124*, 519–529. https://doi.org/10.1182/blood-2014-03-565721.

Cho, S.W., Soki, F.N., Koh, A.J., Eber, M.R., Entezami, P., Park, S.I., van Rooijen, N., and McCauley, L.K. (2014). Osteal macrophages support physiologic skeletal remodeling and anabolic actions of parathyroid hormone in bone. Proc. Natl. Acad. Sci. USA *111*, 1545–1550. https://doi.org/10.1073/pnas.1315153111.

Chow, A., Huggins, M., Ahmed, J., Hashimoto, D., Lucas, D., Kunisaki, Y., Pinho, S., Leboeuf, M., Noizat, C., van Rooijen, N., et al. (2013). CD169(+) macrophages provide a niche promoting erythropoiesis under homeostasis and stress. Nat. Med. *19*, 429–436. https://doi.org/10.1038/nm.3057.

Degen, W.G., van Kempen, L.C., Gijzen, E.G., van Groningen, J.J., van Kooyk, Y., Bloemers, H.P., and Swart, G.W. (1998). MEMD, a new cell adhesion molecule in metastasizing human melanoma cell lines, is identical to ALCAM (activated leukocyte cell adhesion molecule). Am. J. Pathol. *152*, 805–813.

Edgar, R., Domrachev, M., and Lash, A.E. (2002). Gene Expression Omnibus: NCBI gene expression and hybridization array data repository. Nucleic Acids. Res. *30*, 207–210.

Ghosh, J., Mohamad, S.F., and Srour, E.F. (2019). Isolation and Identification of Murine Bone Marrow-Derived Macrophages and Osteomacs from Neonatal and Adult Mice. Methods Mol. Biol. *2002*, 181–193. https://doi.org/10.1007/7651_2018_196.

Huang, R.P., Ozawa, M., Kadomatsu, K., and Muramatsu, T. (1990). Developmentally regulated expression of embigin, a member of the immunoglobulin superfamily found in embryonal carcinoma cells. Differentiation *45*, 76–83.

Huang, R.P., Ozawa, M., Kadomatsu, K., and Muramatsu, T. (1993). Embigin, a member of the immunoglobulin superfamily expressed in embryonic cells, enhances cell-substratum adhesion. Dev. Biol. *155*, 307–314. https://doi.org/10.1006/dbio.1993.1030.

Kacena, M.A., Eleniste, P.P., Cheng, Y.H., Huang, S., Shivanna, M., Meijome, T.E., Mayo, L.D., and Bruzzaniti, A. (2012). Megakaryocytes regulate expression of Pyk2 isoforms and caspase-mediated cleavage of actin in osteoblasts. J. Biol. Chem. *287*, 17257–17268. https://doi.org/10.1074/jbc.M111.309880.

Kacena, M.A., Shivdasani, R.A., Wilson, K., Xi, Y., Troiano, N., Nazarian, A., Gundberg, C.M., Bouxsein, M.L., Lorenzo, J.A., and Horowitz, M.C. (2004). Megakaryocyte-osteoblast interaction revealed in mice deficient in transcription factors GATA-1 and NF-E2. J. Bone Miner. Res. *19*, 652–660. https://doi.org/10.1359/jbmr.0301254.

Layer, J.H., Christy, M., Placek, L., Unutmaz, D., Guo, Y., and Davé, U.P. (2020). LDB1 Enforces Stability on Direct and Indirect Oncoprotein Partners in Leukemia. Mol. Cell Biol. *40*, e00652-19. https://doi.org/10.1128/mcb.00652-19.

Lehmann, J.M., Riethmüller, G., and Johnson, J.P. (1989). MUC18, a marker of tumor progression in human melanoma, shows sequence similarity to the neural cell adhesion molecules of the immunoglobulin superfamily. Proc. Natl. Acad. Sci. USA *86*, 9891–9895. https://doi.org/10.1073/pnas.86.24.9891.

Malinge, S., Thiollier, C., Chlon, T.M., Doré, L.C., Diebold, L., Bluteau, O., Mabialah, V., Vainchenker, W., Dessen, P., Winandy, S., et al. (2013). Ikaros inhibits megakaryopoiesis through functional interaction with GATA-1 and NOTCH signaling. Blood *121*, 2440–2451. https://doi.org/10.1182/blood-2012-08-450627.

McGrath, K.E., Frame, J.M., and Palis, J. (2015). Early hematopoiesis and macrophage development. Semin. Immunol. *27*, 379–387. https://doi.org/10.1016/j.smim.2016.03.013.

Millard, S.M., Heng, O., Opperman, K.S., Sehgal, A., Irvine, K.M., Kaur, S., Sandrock, C.J., Wu, A.C., Magor, G.W., Batoon, L., et al. (2021). Fragmentation of tissue-resident macrophages during isolation confounds analysis of single-cell preparations from mouse hematopoietic tissues. Cell Rep. *37*, 110058. https://doi.org/10.1016/j.celrep.2021.110058.

Mohamad, S.F., Gunawan, A., Blosser, R., Childress, P., Aguilar-Perez, A., Ghosh, J., Hong, J.M., Liu, J., Kanagasabapathy, D., Kacena, M.A., et al. (2021). Neonatal Osteomacs and Bone Marrow Macrophages Differ in Phenotypic Marker Expression

and Function. J. Bone Miner. Res. *36*, 1580–1593. https://doi.org/10.1002/jbmr.4314.

Mohamad, S.F., Xu, L., Ghosh, J., Childress, P.J., Abeysekera, I., Himes, E.R., Wu, H., Alvarez, M.B., Davis, K.M., Aguilar-Perez, A., et al. (2017). Osteomacs interact with megakaryocytes and osteoblasts to regulate murine hematopoietic stem cell function. Blood Adv. *1*, 2520–2528. https://doi.org/10.1182/bloodadvances.2017011304.

Mosley, A.L., Florens, L., Wen, Z., and Washburn, M.P. (2009). A label free quantitative proteomic analysis of the Saccharomyces cerevisiae nucleus. J. Proteonomics *72*, 110–120. https://doi.org/10.1016/j.jprot.2008.10.008.

Silberstein, L., Goncalves, K.A., Kharchenko, P.V., Turcotte, R., Kfoury, Y., Mercier, F., Baryawno, N., Severe, N., Bachand, J., Spencer, J.A., et al. (2016). Proximity-Based Differential Single-Cell Analysis of the Niche to Identify Stem/Progenitor Cell Regulators. Cell Stem Cell *19*, 530–543. https://doi.org/10.1016/j.stem.2016.07.004.

Smeets, M.F.M.A., Chan, A.C., Dagger, S., Bradley, C.K., Wei, A., and Izon, D.J. (2013). Fli-1 Overexpression in Hematopoietic Progenitors Deregulates T Cell Development and Induces Pre-T Cell Lymphoblastic Leukaemia/Lymphoma. PLoS One *8*, e62346. https://doi.org/10.1371/journal.pone.0062346.

Wan, C., Chang, W., Zhang, Y., Shah, F., Lu, X., Zang, Y., Zhang, A., Cao, S., Fishel, M.L., Ma, Q., and Zhang, C. (2019). LTMG: a novel statistical modeling of transcriptional expression states in single-cell RNA-Seq data. Nucleic Acids Res. *47*, e111. https://doi.org/10.1093/nar/gkz655.

Watkins, D.S., True, J.D., Mosley, A.L., and Baucum, A.J., 2nd. (2018). Proteomic Analysis of the Spinophilin Interactome in Rodent Striatum Following Psychostimulant Sensitization. Proteomes *6*, 53. https://doi.org/10.3390/proteomes6040053.

Wilson, M.C., Kraus, M., Marzban, H., Sarna, J.R., Wang, Y., Hawkes, R., Halestrap, A.P., and Beesley, P.W. (2013). The neuroplastin adhesion molecules are accessory proteins that chaperone the monocarboxylate transporter MCT2 to the neuronal cell surface. PLoS One *8*, e78654. https://doi.org/10.1371/journal.pone.0078654.

Winkler, I.G., Sims, N.A., Pettit, A.R., Barbier, V., Nowlan, B., Helwani, F., Poulton, I.J., van Rooijen, N., Alexander, K.A., Raggatt, L.J., and Lévesque, J.P. (2010). Bone marrow macrophages maintain hematopoietic stem cell (HSC) niches and their depletion mobilizes HSCs. Blood *116*, 4815–4828. https://doi.org/10.1182/blood-2009-11-253534.

Xu, L., Mohammad, K.S., Wu, H., Crean, C., Poteat, B., Cheng, Y., Cardoso, A.A., Machal, C., Hanenberg, H., Abonour, R., et al. (2016). Cell Adhesion Molecule CD166 Drives Malignant Progression and Osteolytic Disease in Multiple Myeloma. Cancer Res. *76*, 6901–6910. https://doi.org/10.1158/0008-5472.CAN-16-0517.

Yona, S., Kim, K.-W., Wolf, Y., Mildner, A., Varol, D., Breker, M., Strauss-Ayali, D., Viukov, S., Guilliams, M., Misharin, A., et al. (2013). Fate Mapping Reveals Origins and Dynamics of Monocytes and Tissue Macrophages under Homeostasis. Immunity *38*, 79–91. https://doi.org/10.1016/j.immuni.2012.12.001.

Zhang, J., Ghosh, J., Mohamad, S.F., Zhang, C., Huang, X., Capitano, M.L., Gunawan, A.M., Cooper, S., Guo, B., Cai, Q., et al. (2019). CD166 Engagement Augments Mouse and Human Hematopoietic Progenitor Function via Activation of Stemness and Cell Cycle Pathways. Stem Cell. *37*, 1319–1330. https://doi.org/10.1002/stem.3053.

Zhang, J., Niu, C., Ye, L., Huang, H., He, X., Tong, W.G., Ross, J., Haug, J., Johnson, T., Feng, J.Q., et al. (2003). Identification of the haematopoietic stem cell niche and control of the niche size. Nature *425*, 836–841.

Zhu, H., Traver, D., Davidson, A.J., Dibiase, A., Thisse, C., Thisse, B., Nimer, S., and Zon, L.I. (2005). Regulation of the lmo2 promoter during hematopoietic and vascular development in zebrafish. Dev. Biol. *281*, 256–269. https://doi.org/10.1016/j.ydbio.2005.01.034.